The Astrophysical Journal, 598:1217–1228, 2003 December 1

WHITE DWARF DONORS IN ULTRACOMPACT BINARIES: THE STELLAR STRUCTURE OF FINITE-ENTROPY OBJECTS

Christopher J. Deloye
Department of Physics, Broida Hall, University of California, Santa Barbara, CA 93106;
cjdeloye@physics.ucsb.edu

and

Lars Bildsten
Kavli Institute for Theoretical Physics and Department of Physics, Kohn Hall, University of California, Santa Barbara, CA 93106;
bildsten@kitp.ucsb.edu
Received 2003 June 12; accepted 2003 August 12

ABSTRACT

We discuss the mass-radius (M-R) relations for low-mass ($M < 0.1\ M_\odot$) white dwarfs (WDs) of arbitrary degeneracy and evolved (He, C, O) composition. We do so with both a simple analytical model and models calculated by integration of hydrostatic balance using a modern equation of state valid for fully ionized plasmas. The M-R plane is divided into three regions where either Coulomb physics, degenerate electrons, or a classical gas dominates the WD structure. For a given M and central temperature T_c, the M-R relation has two branches differentiated by the model's entropy content. We present the M-R relations for a sequence of constant-entropy WDs of arbitrary degeneracy parameterized by M and T_c for pure He, C, and O. We discuss the applications of these models to the recently discovered accreting millisecond pulsars. We show the relationship between the orbital inclination for these binaries and the donor's composition and T_c. In particular, we find from orbital inclination constraints that the probability XTE J1807−294 can accommodate a He donor is approximately 15%, while for XTE J0929−304 it is approximately 35%. We argue that if the donors in ultracompact systems evolve adiabatically, there should be 60–160 more systems at orbital periods of 40 minutes than at orbital periods of 10 minutes, depending on the donor's composition. Tracks of our mass-radius relations for He, C, and O objects are available in the electronic version of this paper.

Subject headings: binaries: close — pulsars: individual (XTE J0929−314, XTE J1751−305, XTE J1807−294) — white dwarfs — X-rays: binaries

On-line material: source code

1. INTRODUCTION

The discovery of three X-ray transient ultracompact accreting millisecond pulsars (MSPs), XTE J1751−305 (Markwardt et al. 2002), XTE J0929−314 (Galloway et al. 2002), and XTE J1807−294 (Markwardt, Juda, & Swank 2003a; Markwardt, Smith, & Swank 2003b) have demonstrated the existence of binary pulsar systems with low-mass ($M_2 \approx 10^{-2}\ M_\odot$) donors. These three ultracompact systems (here defined as binaries with orbital periods $P_{\rm orb} < 60$ minutes) are remarkably homogeneous, with measured $P_{\rm orb}$ values of 42.4, 43.6, and 40.1 minutes, respectively, well below the minimum period for a system with a donor composed primarily of hydrogen (Rappaport, Joss, & Webbink 1982). Since the nature of the donors in these systems today depends on the prior evolution of the system, it is useful to discuss the potential formation mechanisms for these systems.

Binary systems with $P_{\rm orb} < 80$ minutes can form through at least two channels. Stable mass transfer from an evolved main-sequence star (Nelson, Rappaport, & Joss 1986; Fedorova & Ergma 1989; Podsiadlowski, Rappaport, & Pfahl 2002; Nelson & Rappaport 2003) or a He-burning star (Savonije, de Kool, & van den Heuvel 1986) onto a neutron star (NS) is one mechanism. In this scenario, the main-sequence star is brought into Roche lobe (RL) contact because of orbital angular momentum losses from magnetic braking at a time when the core has nearly completed H burning. Such a system will evolve to orbital periods comparable to the ultracompact MSPs and can reach $P_{\rm orb} \approx 10$ minutes (Podsiadlowski et al. 2002; Nelson & Rappaport 2003). Podsiadlowski et al. (2002) and Nelson & Rappaport (2003) show that the resulting ultracompact binaries have donor masses $M_2 \approx 0.1$–$0.2\ M_\odot$ as they pass through $P_{\rm orb} \approx 40$ minutes on their way toward a shorter period. These masses are significantly greater than those measured in the ultracompact MSPs (Galloway et al. 2002; Markwardt et al. 2002; Bildsten 2002). However, systems evolving through 40 minutes on the way out from the period minimum have masses more in line with the measurements ($M_2 \approx 0.01\ M_\odot$), and by this time the donors have become partially degenerate with core temperatures $T_c \sim 10^5$–10^6 K (Nelson & Rappaport 2003).

The second scenario that may form ultracompact systems involves triggering a common-envelope phase during an unstable mass transfer episode from the donor onto the NS. The core of the donor, either a He or C/O white dwarf (WD), and the NS spiral-in to shorter orbital periods until the envelope is expelled (Paczyński 1976). Several authors have proposed binary evolution scenarios in which the system, after emerging from the common-envelope phase, suffers in-spiral because of gravitational wave (GW) emission and eventually reestablishes contact (Iben & Tutukov 1985; Rasio, Pfahl, & Rappaport 2000; Dewi et al. 2002;

Yungelson, Nelemans, & van den Heuvel 2002). During this long GW in-spiral, the WD will have had time to cool, setting the entropy of the donor at the onset of the second mass transfer phase (Bildsten 2002). Tauris (1996) finds that a large fraction of the NS-WD binaries that undergo a common-envelope phase will reach contact within 1 Gyr. Even considering a longer 4 Gyr delay between the formation of the WD secondary and the onset of mass transfer, a He WD will have $T_c \approx 3 \times 10^6$ to 10^7 K (Althaus & Benvenuto 1997; Driebe et al. 1999; Serenelli et al. 2001), while a C/O WD will have $T_c \approx (2\text{–}3) \times 10^6$ K (Salaris et al. 2000). The mass transfer timescale at contact is much shorter than the WD cooling timescale for these WDs, so the initial entropy of these objects is the minimum attainable. As noted by Bildsten (2002), if these objects adiabatically expand under mass loss, their T_c-values will have been reduced by a factor of $\approx$15 by the time they have reached $M_2 \approx 0.01\ M_\odot$.

In addition to the evolutionary arguments that donors in the ultracompact MSPs have not reached a $T = 0$ configuration, the system XTE J1751−305 provides observational evidence for a hot donor since, as noted by Bildsten (2002), a fully degenerate companion composed of He or C cannot fill its RL in this system. Hence, in examining the donors in the ultracompact accreting MSPs, we need to consider them to be arbitrarily degenerate low-mass objects of evolved (He or C/O) composition. To further constrain the nature of these donors (for example, their T_c) requires knowledge of their mass-radius (M-R) relation. For the compositions (He, C/O) and mass ($\sim$0.01 $M_\odot$) and T_c ($\sim 10^5$–10^7 K) ranges of relevance to these objects, the corresponding central densities ($\rho_c \sim 10^3$ g cm^{-3}) are such that Coulomb and thermal contributions to the equation of state (EOS) provide nonnegligible corrections to the degenerate electron pressure, impacting their M-R relations. In this paper, we detail the M-R relation for low-mass stellar objects of finite T_c, extending the M-R relations of Zapolsky & Salpeter (1969) for $T = 0$ objects. In particular, we make clear that there is a *continuous connection* between fully degenerate objects (i.e., WDs), fully convective low-mass stars (i.e., $n = 3/2$ polytropes), and Coulomb-dominated objects.

We begin in § 2.1 by constructing a simple model of these objects using an approximate EOS. Although crude, this model describes adequately the relevant physics and yields an analytic description of the qualitative behavior of the M-R relations and how they are affected by Coulomb and thermal contributions to the EOS. We find that at finite T_c, arbitrarily degenerate sequences exhibit a two-branch solution, a fact noted previously (e.g., Cox & Guili 1968; Cox & Salpeter 1964; Hansen & Spangenberg 1971; Rappaport & Joss 1984). Further, for sufficiently high values of T_c, the sequence of solutions on these two branches exhibits a mutual endpoint at a *nonzero mass* $M_{\rm min}$, below which equilibrium solutions do not exist. When Coulomb contributions are small and electrons are nonrelativistic, fully convective stellar models of arbitrary degeneracy are well represented by $n = 3/2$ polytropes (Hayashi & Nakano 1963; Stevenson 1991; Burrows & Liebert 1993; Ushomirsky et al. 1998). In § 2.2 we review the role played by degeneracy in determining the M-R relation for $n = 3/2$ polytropes and the existence of a two-branch solution for the polytrope M-R relation. Other authors have noted that for a given M, there is a maximum T_c that such polytrope models may have (Cox & Guili 1968; Rappaport & Joss 1984; Stevenson 1991; Burrows & Liebert 1993; Ushomirsky et al. 1998). We connect the existence of a maximum T_c with that of $M_{\rm min}$. In § 2.3 we construct realistic M-R relations using an EOS for fully ionized plasmas. There we exhibit explicitly the impact of Coulomb physics on the M-R relations. Like the simplified and polytrope models, we find that the M-R relations of this model exhibit a two-branch solution and a nonzero $M_{\rm min}$ at high values of T_c.

In § 3 we apply our stellar models to the ultracompact MSP systems. For each of these systems, there is a donor (of some composition and T_c) which will fill the RL at the required $P_{\rm orb}$ for any given orbital inclination. Also, for a given composition, there is in each system a relation between orbital inclination and T_c. We examine what constraints this places on the composition and T_c of the donors in these systems. For example, in XTE J1807−294, C and He donors can have any T_c, while an O donor's T_c has a minimum value. In XTE J1751−305, all He or C/O donors must be hot. We also examine how the future evolution of these systems depends on donor composition and T_c and highlight the fact that a multiple-valued M-R relation leads to a multiple-valued relation between $P_{\rm orb}$ and the system's mass transfer rate $\dot{M}$. Finally, in the context of adiabatic evolution, we discuss the expected number distribution of ultracompact systems as a function of $P_{\rm orb}$. In a steady state, this distribution depends almost solely on the response of the donor radius R_2 to mass loss through the quantity $n_R \equiv d \ln R_2 / d \ln M_2$. The increased importance of Coulomb physics in C/O donors alters n_R as compared to He donors, and the expected distribution for the two donor types differs dramatically. Depending on donor type, the relative number of systems at $P_{\rm orb} \approx 40$ minutes as compared to those at $P_{\rm orb} \approx 10$ minutes is $\approx$60 for He donors and $\approx$160 for C/O donors. We conclude in § 5 by discussing future applications of and refinements to our models.

2. MASS-RADIUS RELATIONS FOR LOW-MASS ARBITRARILY DEGENERATE STARS

In the mass range of interest ($M_2 < 0.1\ M_\odot$), M-R relations for various objects have previously been constructed. For H-rich objects, Burrows et al. (2001) summarize the work that has been done on the structure and evolution of brown dwarfs and related objects. For these objects, the models include detailed treatment of the EOS and atmospheric physics. On the other hand, for objects with more evolved composition (i.e., He or C/O), the theory is not so mature. Zapolsky & Salpeter (1969) calculated the M-R relations for $T = 0$ objects using the EOS they derived from the Thomas-Fermi-Dirac equation (Salpeter & Zapolsky 1967). This EOS treats in an approximate manner the corrections due to Coulomb interactions and exchange effects in a fully degenerate plasma. Additional M-R relations produced by several different $T = 0$ EOSs are presented in Lai, Abrahams, & Shapiro (1991) but do not differ appreciably from the Salpeter & Zapolsky (1967) results. For the partially degenerate case, there is a large body of literature for He- and C/O-core WDs more massive than 0.1 $M_\odot$ (Fontaine, Brassard, & Bergeron 2001; Panei, Althaus, & Benvenuto 2000), but only recently have M-R relations for arbitrarily degenerate He and C/O WDs with masses less than 0.1 $M_\odot$ been calculated (Bildsten 2002), and only for a limited number of cases. Here we fill this gap by constructing low-mass WD models utilizing a realistic EOS.

2.1. *A Simple Model for Arbitrarily Degenerate Stars*

Degenerate stellar objects with $10^{-3} \lesssim M/M_\odot \lesssim 10^{-2}$ have central densities $\rho_c \sim 10^2$–10^3 g cm^{-3}. In this density range, the relative energy contributions to the plasma from an ideal Fermi gas and Coulomb interactions can be comparable. Also, for these densities, at a temperature $T \sim 10^6$ K, the thermal contributions to the pressure are about 10% of those of the electrons. At lower densities, Coulomb and thermal effects become even more significant in calculating the EOS. To examine the interplay between these contributions and how they impact the structure of low-mass stars, we start with a simple EOS for a plasma composed of ions with charge number Z and atomic mass number A,

$$P(\rho, T) = P_e(\rho) + P_{\rm id}(\rho, T) + P_{\rm C}(\rho) \ , \qquad (1)$$

where P_e is the pressure of a fully degenerate noninteracting Fermi gas of electrons, $P_e = K_e \rho^{5/3}$, $P_{\rm id}$ is the pressure of an ideal gas of ions and electrons, $P_{\rm id} = K_{\rm id} \rho T$, and $P_{\rm C}$ is the negative pressure contribution due to Coulomb interactions in the Wigner-Seitz approximation, $P_{\rm C} = -K_{\rm C} \rho^{4/3}$. Here $K_e = 3.323 \times 10^{12} (2/\mu_e)^{5/3}$ dynes cm^3 g$^{-5/3}$ (μ_e is the mean molecular weight per electron and equals A/Z in a single composition plasma), $K_{\rm id} = 8.25 \times 10^7 (1 + Z)/A$ dynes cm g^{-1}K^{-1}, and $K_{\rm C} = 2.23 \times 10^{12} Z^{2/3} (2/\mu_e)^{4/3}$ dynes cm^2 g$^{-4/3}$.

Consider a one-zone stellar model, i.e., a spherical system characterized by a single pressure and density, P and ρ. From dimensional analysis, $P \sim GM^2/R^4$ and $\rho \sim M/R^3$, where M and R are the mass and radius of the star and G is the Newtonian constant of gravitation. With the pressure given by equation (1),

$$G \frac{M^2}{R^4} \approx K_{\rm id} T \frac{M}{R^3} + K_e \frac{M^{5/3}}{R^5} - K_{\rm C} \frac{M^{4/3}}{R^4} \qquad (2)$$

In the $T \to 0$ limit, the term involving $K_{\rm id}$ vanishes, and solving for R gives

$$R(T = 0) = \frac{K_e M^{1/3}}{K_{\rm C} + G M^{2/3}} \ , \qquad (3)$$

showing that the gravitational and Coulomb attractions act to collapse the star, which is supported by the degenerate electron pressure. As $M \to 0$, Coulomb forces dominate gravity and $R \propto M^{1/3}$. As $M \to \infty$, Coulomb forces become negligible and $R \propto M^{-1/3}$. The transition from a gravitational to a Coulomb-dominated regime occurs where $M \sim (K_{\rm C}/G)^{3/2} \sim 10^{-4} Z (2/\mu_e)^2 \, M_\odot$. The relation $R \propto M^{1/3}$ in the low-M limit implies a constant density $\rho_{\rm min}$ fixed by the balance between the electron pressure and Coulomb attraction. Exhibiting ρ explicitly as a function of M, $\rho = (GM^{2/3} + K_{\rm C})/K_e$ and $\rho_{\rm min} = (K_{\rm C}/K_e)^3 = 0.671 Z^2$ g cm^{-3}.

For $T > 0$, equation (2) has solutions given by

$$R = \frac{M^{1/3}}{2K_{\rm id} T} \left[K_{\rm C} + G M^{2/3} \pm \sqrt{(K_{\rm C}^2 - 4K_e K_{\rm id} T) + 2K_{\rm C} G M^{2/3} + G^2 M^{4/3}} \right] . \qquad (4)$$

Figure 1 exhibits several isotherms of the M-R relation of equation (4). The two-branch nature of this relation is apparent, as is the clear separation into three classes of stellar objects. The large-M lower branch is made up of gravitationally bound objects supported by degeneracy pressure. On the lower branch at small M, we have Coulomb-dominated objects. The upper branch consists of objects supported by thermal pressure.

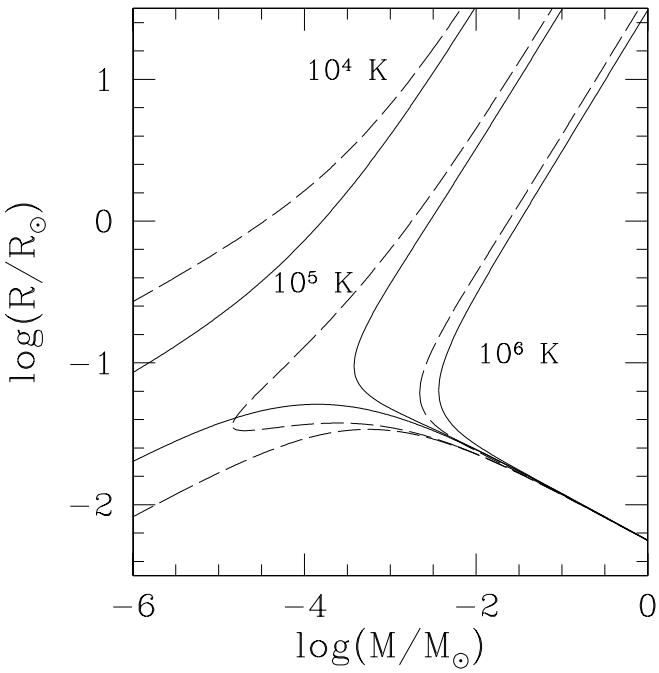

FIG. 1.—Schematic M-R relation of our simple model given by eq. (5). The curves show isotherms at $T = 10^4$, 10^5, and 10^6 K for pure He (*solid curves*) and C (*dashed curves*) compositions. The curves on the upper branch are labeled with their respective temperatures. The lower branch curves at low M have $T = 10^4$ K.

For $T > 0$, there exists a minimum mass $M_{\rm min}$ found by setting the discriminant in equation (5) to zero,

$$M_{\rm min} = \frac{2(K_e K_{\rm id} T)^{1/2} - K_{\rm C}}{G} \ . \qquad (5)$$

This expression is positive only if $T > 4.53 \times 10^3 A Z^{4/3}/(1 + Z)(2/\mu_e)$ K. For He (C) this temperature is 1.5×10^4 (8.5×10^4) K. Above this critical temperature, the two branches meet at a mutual endpoint and no solution with $M < M_{\rm min}$ exists. When Coulomb physics is negligible, $M_{\rm min}$ occurs at the point where $P_e = P_{\rm id}$ along the solution curve. The existence of $M_{\rm min}$ results from the fact that for $M < M_{\rm min}$, the pressure provided by $P_e + P_{\rm id}$ at any ρ is greater than that needed to support the star (this is not the case for either an ideal gas or a Fermi gas independent of the other; in either of these cases it is well known that equilibrium solutions down to $M = 0$ exist). Alternately, for a given M, the isotherm on which $M = M_{\rm min}$ gives the maximum T for which solutions exist with this mass. For an object starting out on an upper branch solution, e.g., a recently expired star, as it loses entropy via radiation, it contracts. For a fixed mass, a star supported by thermal pressure has $T \propto R^{-1}$ and it heats up, as expected. The thermal pressure in this case goes as $P_{\rm id} \propto R^{-4}$, but $P_e \propto R^{-5}$ and eventually P_e dominates, halting substantial contraction.

Further entropy loss leads to a reduction in T. For a given T and M, the two possible solutions are physically distinguished by their entropy.

2.2. *Polytrope Models for Low-Mass Stars Neglecting Coulomb Physics*

Ignoring nonideal effects and assuming that the electrons are nonrelativistic, a fully convective object has an EOS obeying $P \propto \rho^{5/3}$ and is modeled by an $n = 3/2$ polytrope. The specific entropy s throughout such a model is a constant. Since s depends only on the degeneracy parameter η, defined as the ratio of the chemical potential of the electrons to kT (k being the Boltzmann constant), η is also a constant of the model (Ushomirsky et al. 1998). Following Ushomirsky et al. (1998), this allows us to write the pressure of a noninteracting gas of electrons and ions as

$$P = \frac{\rho}{\mu_{\rm eff} m_p} kT \ , \tag{6}$$

where m_p is the mass of a proton and $\mu_{\rm eff}$ is defined as

$$\frac{1}{\mu_{\rm eff}} = \frac{1}{\mu_i} + \frac{2F_{3/2}(\eta)}{3\mu_e F_{1/2}(\eta)} \ , \tag{7}$$

thus varying as η changes. Here μ_i is the ion mean molecular weight and F_k is the Fermi-Dirac function of order k from Cox & Guili (1968). We then utilize the $n = 3/2$ polytrope relations, equation (6), and the fact that $F_{1/2}(\eta) \propto \rho/(\mu_e T^{3/2})$ to determine M and R as functions of η and T_c. These results can be expressed as

$$\frac{R}{R_\odot} = 0.359 \left(\frac{M}{0.01\ M_\odot}\right)^{-1/3} (\mu_e^{2/3} \mu_{\rm eff} F_{1/2}^{2/3})^{-1} \ , \tag{8}$$

$$T_c = 3.42 \times 10^5\ {\rm K} \left(\frac{M}{0.01\ M_\odot}\right)^{4/3} (\mu_e^{1/3} \mu_{\rm eff} F_{1/2}^{1/3})^2 \ , \tag{9}$$

which is a minor rewrite of the results in Ushomirsky et al. (1998).

Equation (9) shows the relation between T_c and M is a function of η through the combination $\mu_{\rm eff} F_{1/2}^{1/3}$, which has a single maximum at $\eta \approx 3$–5 for expected WD interior compositions. Just as in the simple models of § 2.1, this shows explicitly the connection between a maximum T_c for a given M and the existence of an $M_{\rm min}$ for a fixed T_c. Here again there are two equilibrium radii for a given M and T_c differentiated by their degree of degeneracy or, equivalently, their entropy.

The transition from a thermal pressure–dominated to degeneracy pressure–dominated state in these models approximately determines $M_{\rm min}$. This transition occurs near where $1/\mu_i \approx 2F_{3/2}/3\mu_e F_{1/2}$. For increasing values of μ_i, this occurs at lower values of η, i.e., at lower values of ρ_c if μ_e and T_c are held fixed. With $P \propto \rho^{5/3}$, dimensional analysis shows $M \propto \rho_c^{1/2}$; a lower density at the transition between degenerate and nondegenerate states gives a smaller $M_{\rm min}$. For a fixed T_c, a pure-C WD will have a smaller $M_{\rm min}$ than a pure-He WD.

2.3. *Mass-Radius Relations for Isentropic White Dwarfs*

We now calculate the M-R relations derived from stellar models that include Coulomb physics. In these calculations, we assume that the interior profiles of our stellar models are adiabatic. In reality, the actual entropy profile in a given donor will depend on its evolutionary history. Many factors—such as whether the system formed through a stable or unstable mass transfer channel, whether or not H burning is still ongoing at the point of contact, and how the mass transfer rate changes with time—can impact either the initial entropy profile of the donor or its subsequent evolution. In calculating models for donors in ultracompact binaries, without choosing their evolutionary history, a reasonable approximation of their internal entropy profile is the best that can be done. Since we aim to construct models that will enable analysis of the donor's properties today, irrespective of their past histories, we must assume some internal profile in calculating them.

A system that initiates mass transfer at $P_{\rm orb} \lesssim 40$ minutes has a donor mass $M_2 \gtrsim 0.01\ M_\odot$. The mass transfer timescale for such a system with an NS primary is roughly $M_2/\dot{M} \lesssim 1$–100 Myr, depending on M_2. Consideration of the flux through the half-mass point in our models due to electron conduction (calculated using the conductive opacities of Potekhin et al. 1999) compared to the heat content of the interior half of the model shows roughly that the time required to transport this heat out of the interior is $\sim$100 Myr to 1 Gyr, again depending on M_2. Thus, during the mass transfer episode that would lead up to the creation of systems at $P_{\rm orb} \approx 40$ minutes, the internal evolution is to first order an adiabatic expansion and, in the absence of tidal heating, the initial entropy profile should be more or less preserved with some corrections due to heat transport. To whatever degree this occurs, the critical point is that the interior will not be able to maintain an isothermal profile. We chose to use an adiabatic profile instead of another arbitrary choice, since it provides several convenient features: it is a limiting case for the possible thermal profiles of the donor and produces the most compact configuration for a given T_c and M_2, it is completely determined by the utilized EOS, and it allows parameterization of a set of models by one quantity, the specific entropy that is constant throughout the model. In addition, the calculations of Nelson & Rappaport (2003) show that He donors tend to become adiabatic as they lose mass. These latter calculations also highlight that throughout the mass loss episode, donors remain far from isothermal except in the deep interior of the star, and then only at masses near 0.1 $M_\odot$ (Nelson & Rappaport 2003).

2.3.1. *Equation of State*

For the EOS, we use the results of Chabrier & Potekhin (1998) and Potekhin & Chabrier (2000). Their work provides accurate prescriptions for calculating the EOS for a fully ionized plasma in either liquid or solid states that includes the ideal contributions from nondegenerate ions and degenerate electrons and the nonideal contributions due to Coulomb interactions. We also include the radiation contribution, a small effect. In the calculations below, we assume that the plasma is in the solid state when the quantity

$$\Gamma \equiv \frac{(Ze)^2}{akT} \gtrsim 173 \tag{10}$$

(Farouki & Hamaguchi 1993). Here a is the inter-ion spacing given by $a = (4\pi n_i/3)^{-1/3}$, n_i being the number density of ions. The quantity Γ is a measure of the strength of the ionic Coulomb interactions. We display a set of isotherms

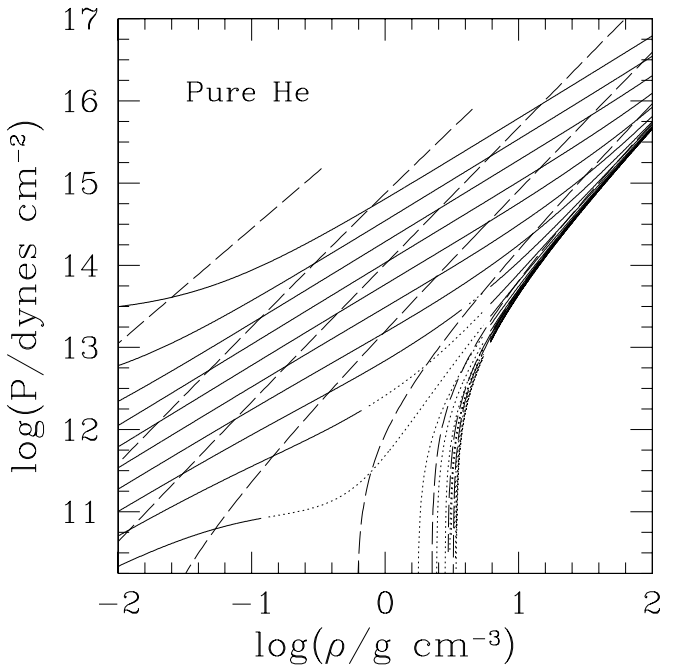

FIG. 2.—He EOS that we utilize showing the comparison isotherms (*solid and dotted lines*) and a set of representative adiabats (*dashed lines*). The isotherms are for temperatures incremented by $\Delta\log(T/\mathrm{K}) = 0.5$, with the upper curves corresponding to $\log(T/\mathrm{K}) = 7$. Along the isotherms, the dotted lines indicate regions where the plasma is not fully ionized. The adiabats typically cross into regions where full ionization of the plasma is not definite and is a source of uncertainty in some of our models.

for a pure-He plasma calculated with this EOS in Figure 2 with the solid and dotted lines. The dotted lines indicate regions in parameter space where T and ρ are such that the plasma will likely become only partially ionized. In these regimes this EOS is not strictly valid.

The dashed lines in Figure 2 show representative adiabats for this EOS, some of which cross into regions of partial ionization. Since we utilize an adiabatic internal profile in calculating our models in § 2.3.2, in some of these models there can be a point in their outer layers where our EOS becomes invalid. We use our EOS in these regimes despite this problem for two reasons: First, in the models of most interest only the very outermost layers of the models lie in regimes where ionization state transitions become an issue and the calculated *M-R* relation is not affected. Second, this EOS provides a simple method of calculating the EOS for various compositions over a wide range of ρ and T, and this ease of use would be sacrificed by constructing composition-specific extensions to the EOS. We highlight in our results models in which these EOS concerns may cause more than a few percent uncertainty in the calculated *M-R* relations.

2.3.2. *Calculation of the Models and Results*

We constructed models for arbitrarily degenerate objects by integrating mass conservation and hydrostatic balance while presuming an adiabatic temperature profile. The calculation of our models proceeds as follows: In the interior, where degeneracy pressure dominates, we integrate

$$\frac{dT}{dr} = \frac{\Gamma_2 - 1}{\Gamma_2}\frac{T}{P}\frac{dP}{dr}\ , \tag{11}$$

where Γ_2 is the adiabatic exponent

$$\frac{\Gamma_2}{\Gamma_2 - 1} = \left(\frac{\partial \ln P}{\partial \ln T}\right)_{\mathrm{ad}} \tag{12}$$

found from the EOS. The density at each integration step is then solved for from P and T using the EOS. At low ρ, where Coulomb effects on the pressure become significant, we switch to integrating

$$\frac{d\rho}{dr} = \frac{1}{\Gamma_1}\frac{\rho}{P}\frac{dP}{dr}\ , \tag{13}$$

where

$$\Gamma_1 = \left(\frac{\partial \ln P}{\partial \ln \rho}\right)_{\mathrm{ad}} \tag{14}$$

is another adiabatic exponent, and solve for T at each integration step from P and ρ. Each model integration was terminated once the following criteria were met: (1) between two integration steps in which P differed by more than a factor of $\approx$20%, m and r changed by no more than 1 part in 10^8, and (2) the current pressure was such that $P/P_c < 10^{-8}$.

We change the integrated variable because as $P \to 0$ along an adiabat, ρ becomes very insensitive to P and it becomes numerically intractable to determine ρ by root-finding from P and T. On the other hand, in the low-P limit, determining T accurately from P and ρ is possible, something that was not true in the highly degenerate regime. We switch from integrating T to integrating ρ when a rough measure of the degeneracy, $167\rho/\mu_e T^{3/2} < 100$, is satisfied (where ρ and T are in cgs units). In the solid state, when $\Gamma \gg 180$, $\Gamma_2 \gg 1$ because of the rapid decline in the plasma's specific heat once crystalline. We use an adaptive step-size, explicit Runge-Kutta algorithm to integrate our equations, with the step size chosen to maintain a fixed fractional accuracy. A dramatic increase in Γ_2 causes a sharp decline in the speed of the integration as the algorithm tries to maintain this accuracy in all three integrated quantities, m, P, and T. To deal with this problem, once $T = 100$ K, we set $dT/dr \approx 0$. This causes no issues in the *M-R* relations because by this point we are already well within the $T \to 0$ limit as far as the *P*-ρ relation is concerned in any of our models.

Finally, in these models the ion coupling parameter Γ increases with r. This is due to the fact that along an adiabat, $\Gamma_3 - 1 = (d\ln T/d\ln\rho)_{\mathrm{ad}}$ varies from $\frac{2}{3}$ to $\approx\frac{1}{2}$ in a Coulomb plasma. Since $\Gamma \propto \rho^{1/3}/T$ and $T \propto \rho^{\Gamma_3 - 1}$, Γ goes as ρ to a negative power. This is true not only for adiabatic profiles; any object with a profile $T \propto \rho^{\gamma}$ for $\gamma > \frac{1}{3}$ will have Γ increasing with r (assuming Z is fixed). Because of this, some models transition from liquid to solid in their outer layers. For these cases we do not attempt to match adiabats in the solid and liquid phase (i.e., we do not account for the latent heat). Instead, the integration assumes continuity of P and T; the entropy in these models has a small discontinuity. If crystallization of the object were to actually occur from the surface inward, this could have significant impact on the mass-loss rate, since the primary's gravitational field would have to overcome the Coulomb binding of the crystal to effect mass transfer. More realistic calculations are obviously needed to consider this further, and consideration of this potential effect in evolutionary calculations is encouraged.

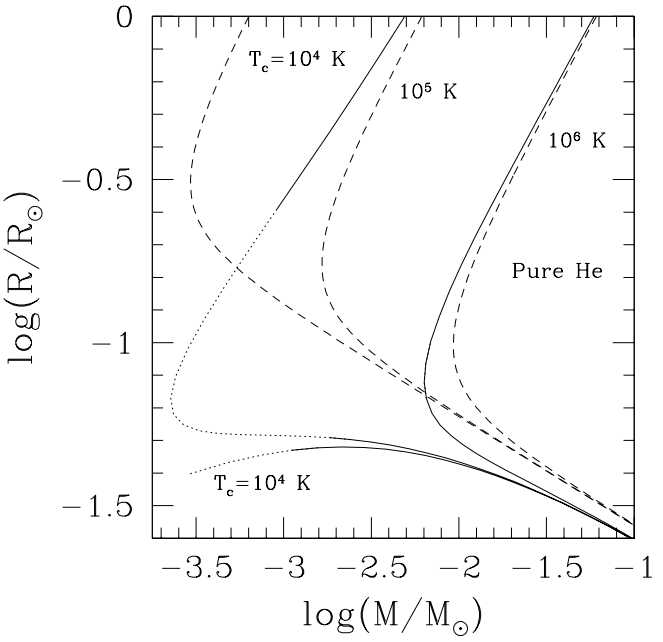

FIG. 3.—Comparison between *M-R* relations for polytropes and the full adiabatic models with Coulomb physics for pure He. The dashed curves show the *M-R* relation for $n = 3/2$ polytropes of pure He at $T_c = 10^4,\ 10^5$, and 10^6 K. The solid curves show He WDs calculated with the full EOS of § 2.3.1 at the same set of T_c as the polytropes. The significance of Coulomb interactions at the masses shown on the *M-R* relation is obvious. The dotted portions of the full curves indicate models where more than 5% of the model's mass is located in regions where the EOS is not strictly valid.

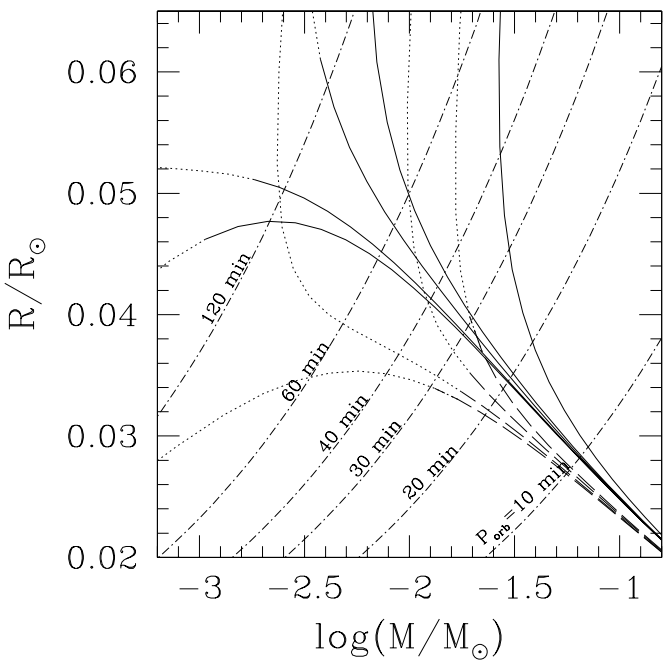

FIG. 4.—*M-R* relations for adiabatic models composed of He (*solid lines*) and C (*dashed lines*). The dotted portions of these curves indicate models where more than 5% of the model by mass is located in regions where the EOS is not strictly valid. The He curves show models with $T_c = 10^2,\ 10^5,\ 5 \times 10^5,\ 10^6$, and 5×10^6 K, and the C curves show models with $T_c = 10^4,\ 10^6,\ 3 \times 10^6$, and 5×10^6 K. The dot-dashed lines are the *M-R* relations for objects filling their RLs at the noted orbital period.

Typical results for our model calculations are shown in Figures 3 and 4. Figure 3 shows for pure-He models how the results utilizing the EOS of § 2.3.1 differ from the polytropes that neglect Coulomb physics. In this figure and in Figure 4 the portions of the *M-R* curves shown in dotted lines indicate models where more than 5% of the mass lies in regions where our EOS is not strictly valid. The impact of Coulomb interactions on the structure of low-mass WDs is clear from the comparison of the He polytrope models (*dashed lines*) with the realistic EOS He models (*solid lines*).

Figure 4 displays a set of *M-R* isotherms for our He (*solid lines*) and C (*dashed lines*) models along with lines of constant $P_{\rm orb}$ for a donor filling its RL overlaid (*dot-dashed lines with* $P_{\rm orb}$ *indicated*). Again, the dotted portions of the *M-R* relations indicate models in which more than 5% of the model's mass lies in a regime where the EOS is not strictly valid. From Figures 3 and 4, it is clear that the realistic treatment of Coulomb physics in the EOS is necessary to calculate accurately the structure of low-mass WDs.

3. APPLICATION OF THE MODELS TO ULTRACOMPACT ACCRETING MILLISECOND PULSARS

We now apply the adiabatic models of § 2.3 to the three known ultracompact accreting MSPs and the high-field X-ray pulsar 4U 1626−67. In Figure 5 we display (*short-dashed lines*) the *M-R* relations of RL-filling donors in XTE J0929−314, XTE J1751−305, and XTE J1807−294 (Markwardt et al. 2002; Galloway et al. 2002; Markwardt et al. 2003a, 2003b) and *M-R* relations for our adiabatic

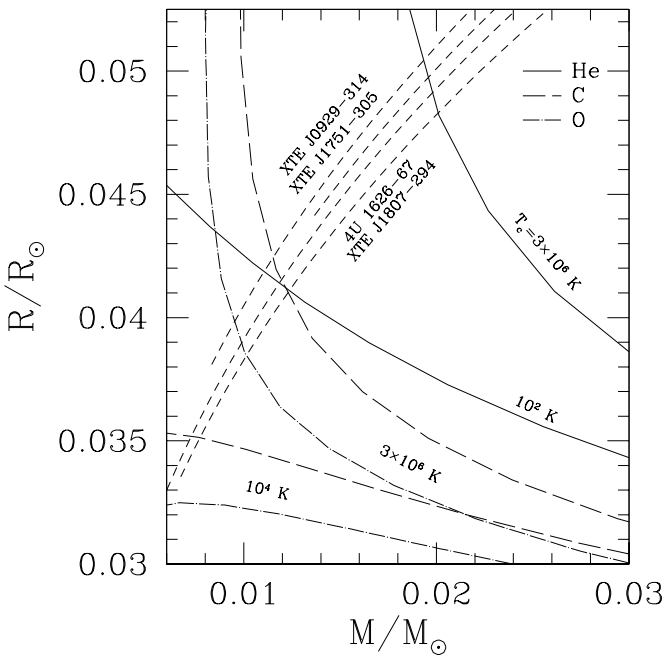

FIG. 5.—Comparison between the *M-R* relations for our adiabatic He (*solid lines*), C (*long-dashed lines*), and O (*dot-dashed lines*) models, along with *M-R* relations for RL-filling donors in the three known accreting MSPs and 4U 1626−67 (*short-dashed lines*). The He *M-R* relations have $T_c = 10^2$ and 3×10^6 K; the C and O have $T_c = 10^4$ and 3×10^6 K. The low T_c relations show approximately the $T = 0$ relation for each composition. The RL-filling solution for 4U 1626−67 extends down to $M = 0$ to indicate that this system has not yet had its mass function measured.

models. We show two isotherms each for He, C, and O models, an approximate $T = 0$ M-R relation and one for hot ($T_c = 3 \times 10^6$ K) models. If the donors in all three systems are He WDs, then $T = 0$ objects are allowed in XTE J0929−314 and XTE J1807−294, but XTE J1751−305 requires a hot donor (Bildsten 2002). For C/O donors, whose M-R relations will lie between the C and O models shown, only XTE J1807−294 permits an RL-filling cold donor. The other two systems both require hot C/O donors. The curves showing the RL-filling M-R relations are parameterized by the orbital inclination i (where $i = 0$ is a face-on system), and there is a correspondence between T_c and i for each donor composition, as shown in Figure 6. From Figure 6, the donor in XTE J1751−305 must have $T_c \gtrsim 10^6$ K. From orbital inclination constraints, the probability that XTE J1807−294 can accommodate a He donor is 15% (for XTE J0929−304, it is ≈35%).

The other ultracompact accreting pulsar, 4U 1626−67, at $P_{\rm orb} = 41.4$ minutes (Middleditch et al. 1981; Chakrabarty 1998) is also shown in Figure 5. Although the orbit has not yet been detected by timing the pulsar, the current upper limit of $a_x \sin i < 8$ lt-ms (Levine et al. 1988; Chakrabarty et al. 1997) allows us, in conjunction with our theoretical work, to constrain the nature of the donor star. Ever since the discovery of a neon emission line (Angelini et al. 1995) from this system, there have been active discussions of the nature of the donor. The Schulz et al. (2001) measurement of a high Ne-to-O ratio (further inferred in other ultracompact binaries by Juett, Psaltis, & Chakrabarty 2001) led them to suggest that the donors in these binaries are the cores of previously crystallized C/O WDs. Homer et al. (2002) have since also seen strong C and O lines but no evidence for helium. Hence, this system seems a likely one to use for probes of C/O donors.

For any $\sin i$, a star that fills the RL at the measured $P_{\rm orb}$ for each of the ultracompact binaries can always be found by some combination of entropy, composition, and mass, and the current values of each impact the orbital evolution of the system. For $M_2/M_1 < 0.8$, the Roche radius R_L can be approximated by (Paczyński 1967)

$$R_L \approx 0.46a\left(\frac{M_2}{M_1 + M_2}\right)^{1/3}, \tag{15}$$

where a is the separation between M_1 and M_2. Combined with Kepler's third law, this leads to the so-called period–mean density relationship,

$$P_{\rm orb} \simeq 8.9 \text{ hr} \left(\frac{R_2}{R_\odot}\right)^{3/2}\left(\frac{M_\odot}{M_2}\right)^{1/2}. \tag{16}$$

Assuming conservative mass transfer, the mass transfer rate (a *positive* quantity) is given by (Verbunt 1993)

$$\frac{\dot{M}}{M_2} = 2\frac{\dot{J}}{J}\frac{1}{n_R + 5/3 - 2M_2/M_1}, \tag{17}$$

where J is the orbital angular momentum, $\dot{J}$ the angular momentum loss rate set by GW emission (Landau &

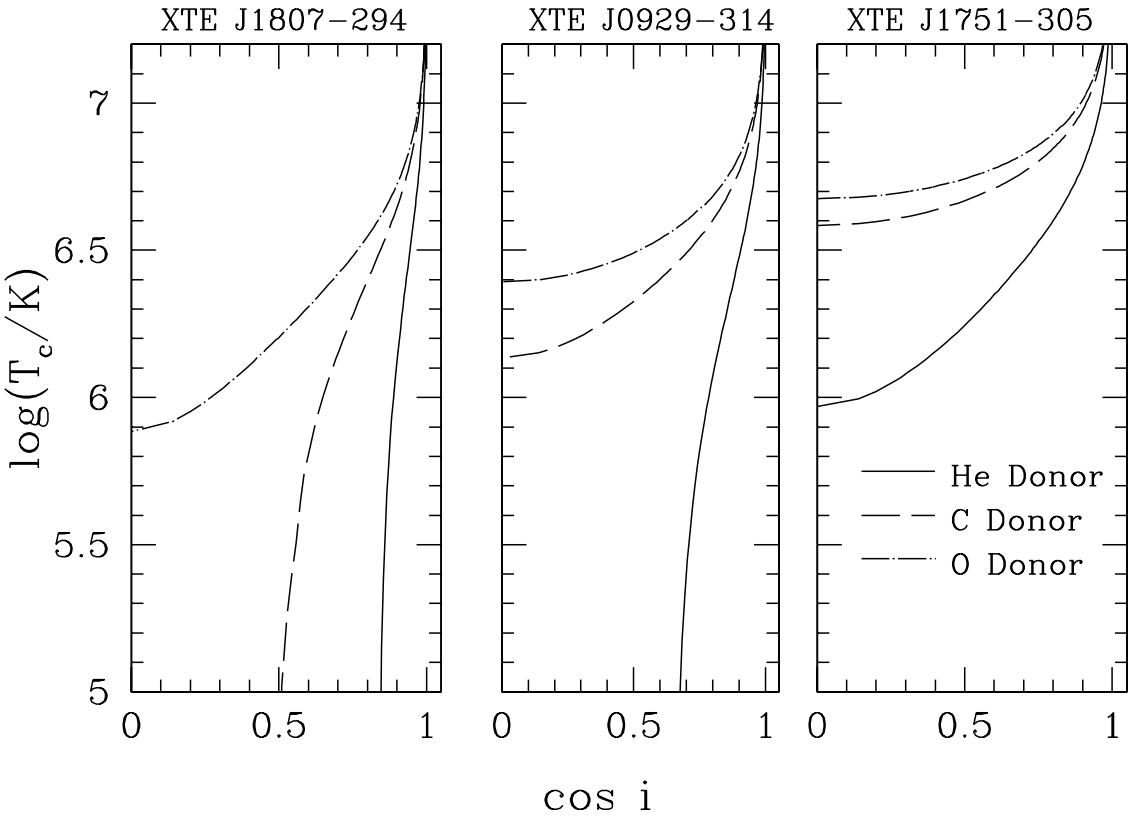

FIG. 6.—Relation between the orbital inclination i and T_c of our adiabatic He, C, and O donors in the ultracompact systems. Hot donors are required in XTE J1751−305 for either He or C/O WD donors; C/O donors in XTE J0929−314 must be hot, while for XTE J1807−294 a $T = 0$ C/O donor is allowed if the system is nearly edge-on.

Lifshitz 1962), and

$$n_R \equiv \frac{d \ln R_2}{d \ln M_2} \ . \tag{18}$$

denotes how the donor's radius changes with mass loss.

For a given system, $\dot{J}$ will depend on the inclination through M_2 and a. The rate at which the orbit evolves will vary accordingly, as will the $\dot{M}$-$P_{\rm orb}$ relation over the course of the evolution. To illustrate this, we calculated the forward evolution of XTE J0929−304 assuming a He donor and four different $\sin i$ values. We assumed that the NS has $M_1 = 1.4\ M_\odot$ (and ignore the change in M_1 due to accretion) and set

$$n_R = n_{\rm ad} \equiv \left(\frac{d \ln R_2}{d \ln M_2} \right)_{\rm ad} , \tag{19}$$

so that the donor evolves adiabatically, ignoring any heating mechanisms (such as irradiation or tidal heating) and cooling. We show the results in Figure 7, displaying M_2 and $\dot{M}$ as a function of $P_{\rm orb}$. These relations are not single valued, but parameterized by orbital inclination or, equivalently, by the donor's entropy. A smaller $\sin i$ requires a more massive donor (which must be hotter than a lower mass donor if it is to have the fixed mean density implied by the system's $P_{\rm orb}$; see also Fig. 6). This gives a higher $\dot{M}$ for a fixed $P_{\rm orb}$, as seen in Figure 7. This also impacts the rate at which the orbit evolves. In Figure 7, the age of the system from today is indicated along each curve by symbols, and it can be seen that the smaller the $\sin i$, the faster the system will evolve in $P_{\rm orb}$.

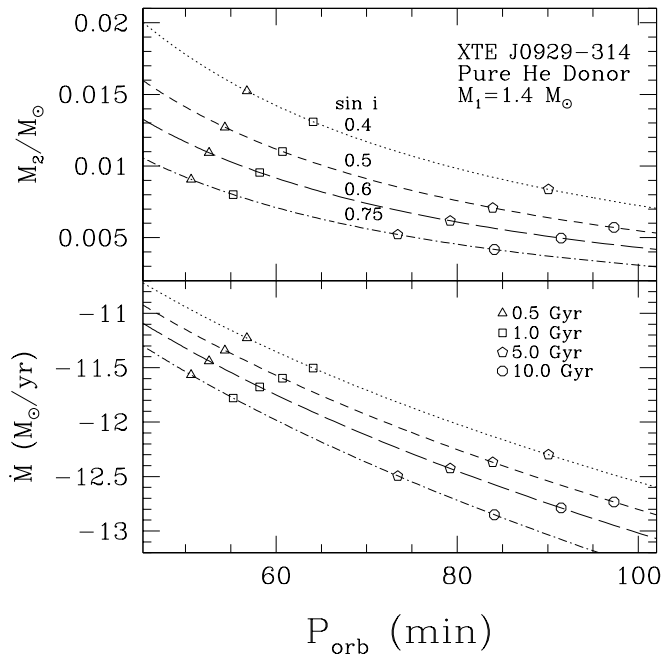

FIG. 7.—Relation between M_2, $\dot{M}$, and $P_{\rm orb}$ for XTE J0929−314 over the course of its orbital evolution forward from today as it depends on $\sin i$ or, equivalently, the entropy of the donor. In particular, the $\dot{M}$-$P_{\rm orb}$ relation is parameterized by the donor's entropy. Along each curve, the symbols designate time from today: *triangles*, 500 Myr; *squares*, 1 Gyr; *pentagons*, 5 Gyr; *circles*, 10 Gyr. A smaller $\sin i$ requires a more massive donor and will produce a faster evolution in $P_{\rm orb}$ for the system.

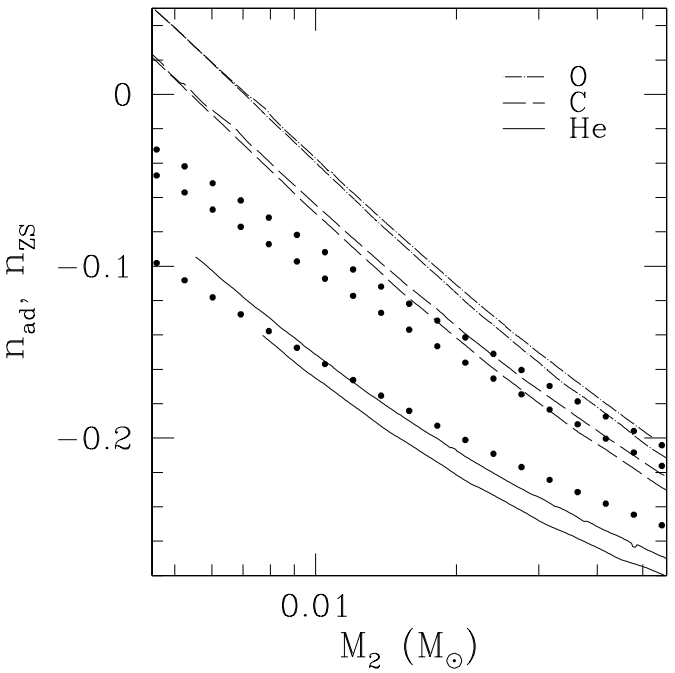

FIG. 8.—Adiabatic change in donor radius with respect to mass, $n_{\rm ad}$, for He (*solid lines*), C (*dashed lines*), and O (*dot-dashed lines*) stars along two representative adiabats for each composition. The lower curve in each set has $T_c = 10^7$ K at the high-mass end; the upper curve has $T_c = 10^2$ K (i.e., it is effectively the $T = 0$ sequence for each composition). The stronger Coulomb physics decreases the magnitude of the radius response to mass loss in the C/O WDs as compared to He WDs. The large dots show n_R for the $T = 0$ Zapolsky-Salpeter models for He, C, and O (*bottom to top*).

At a given orbital inclination in a specified system, a C/O donor must have a higher T_c to fill the RL than a He donor. This is due to the stronger Coulomb physics in the C/O object, which also causes $n_{\rm ad}$ to differ between the donor types and impacts the binary's evolution. The difference in $n_{\rm ad}$ between composition is shown in Figure 8 for two representative adiabatic tracks for each composition. The solid dots show the Zapolsky-Salpeter n_R for the same compositions. The effect of different values of $n_{\rm ad}$ on orbital evolution is evident in Figure 9, which compares the evolution of XTE J0929−304 for $\sin i = 0.6$ and He, C, and O donors. The difference in the tracks comes about because of the difference in $n_{\rm ad}$ due to composition; higher Z donors evolve fastest in mass but slowest in $P_{\rm orb}$ because they remain more dense than lower Z donors at a given mass.

4. THE PERIOD DISTRIBUTION FOR ADIABATICALLY EVOLVING ULTRACOMPACT SYSTEMS

These evolution calculations highlight the dependence of observables ($P_{\rm orb}$ and $\dot{M}$) on the donor's entropy and composition. We now emphasize the impact of the donor composition on the ultracompact population, especially the resulting orbital period distribution. In the scenario of cooling WDs reaching contact via in-spiral (e.g., Nelemans et al. 2001), the relative number of He versus C/O WDs that come into contact and stably reach longer orbital periods is difficult to know. However, what we show here is the ability to constrain the relative populations of, say, He donors, at one orbital period versus another.

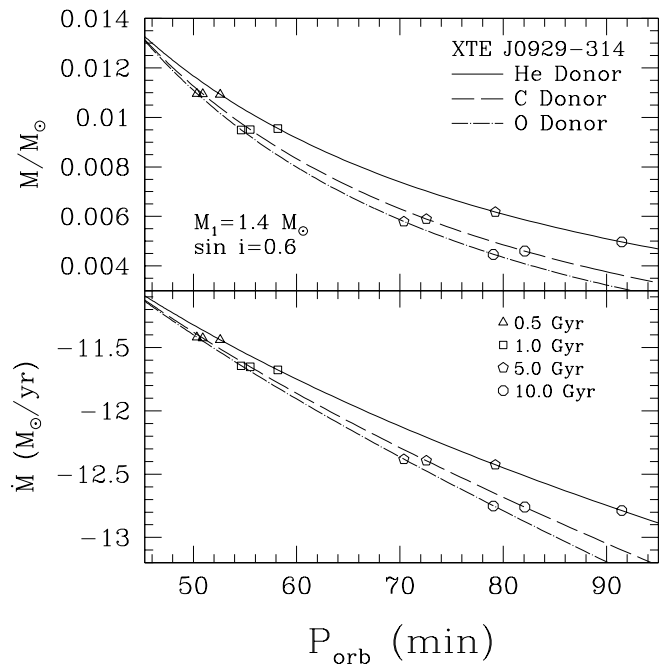

FIG. 9.—Comparison between the evolution of XTE J0929−304 assuming different donor types for an orbital inclination of $\sin i = 0.6$. Shown are M_2 and $\dot{M}$ as a function of $P_{\rm orb}$ for He, C, and O donors. The contrast in the initial evolution between the three donor types comes from the differences in their $n_{\rm ad}$. The symbols mark the age of the system from today.

A more complete picture of this dependence is shown in Figure 10, where we display for He (*solid lines*), C (*dashed lines*), and O (*dot-dashed lines*) donors the $\dot{M}$-$P_{\rm orb}$ relation along M-R isotherms with $T_c = 10^2$, 3×10^6, 10^7, and 3×10^7 K, assuming $M_1 = 1.4\ M_\odot$ and $n = n_{\rm ad}$. These are instantaneous $\dot{M}$-values along an adiabatic track at a given $P_{\rm orb}$ and T_c. One can see immediately that for a given $P_{\rm orb}$, $\dot{M}$ can constrain the combination of donor T_c and composition. In particular, a sufficiently strong upper limit on $\dot{M}$ can *rule out* a He donor for a given $P_{\rm orb}$. Above the minimum $\dot{M}$ for a He donor, further information about the donor composition is difficult to infer without constraints on T_c.

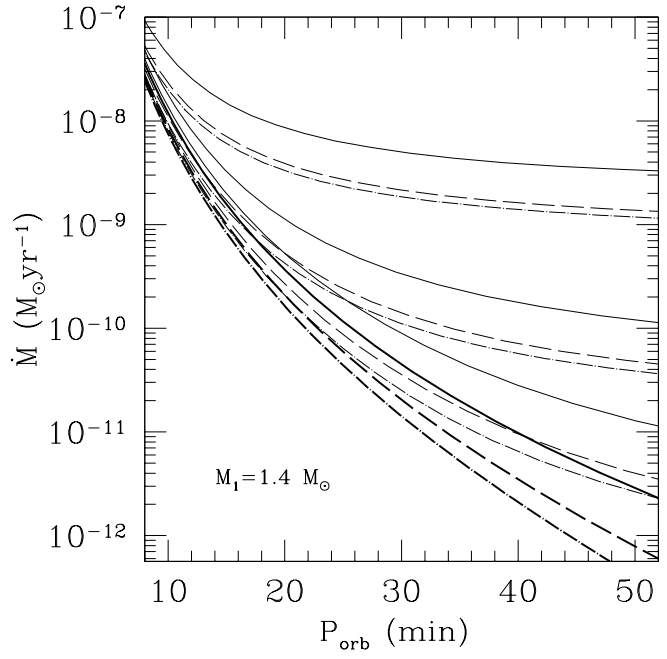

FIG. 10.—$\dot{M}$-$P_{\rm orb}$ relations assuming $n_R = n_{\rm ad}$ for He (*solid lines*), C (*dashed lines*), and O (*dot-dashed lines*). For each composition, the four curves show lines of constant $T_c = 10^2$, 3×10^6, 10^7, and 3×10^7 K (*bottom to top*). The thicker lines are the $T = 10^2$ K curves.

Now consider adiabatic evolution with initial $M_1 = 1.4\ M_\odot$ and donors of varying composition and T_c that fill their RLs at $P_{\rm orb} = 10$ minutes. We evolve these systems assuming the donor responds adiabatically to mass loss. The resulting tracks in the $\dot{M}$-$P_{\rm orb}$ diagram are shown in Figure 11, along with the measured periods of the known ultracompact binaries with an NS primary (*vertical dotted lines*) and the critical $\dot{M}$ below which the accretion disk in these systems is subject to thermal instabilities for both irradiated (*hatched region*; Dubus et al. 1999) and nonirradiated disks (*nearly horizontal lines*; Menou, Perna, & Hernquist 2002). As compared with Figure 10, it can be seen that for systems at $P_{\rm orb} > 30$ minutes to have *time-averaged* mass transfer rates $\dot{M} > 10^{-10}\ M_\odot\ {\rm yr}^{-1}$, the donor cannot have evolved adiabatically from systems coming into contact at $P_{\rm orb} \approx 10$ minutes. There are potentially two examples of such systems: 4U 1626−67 ($P_{\rm orb} = 41.4$ minutes and

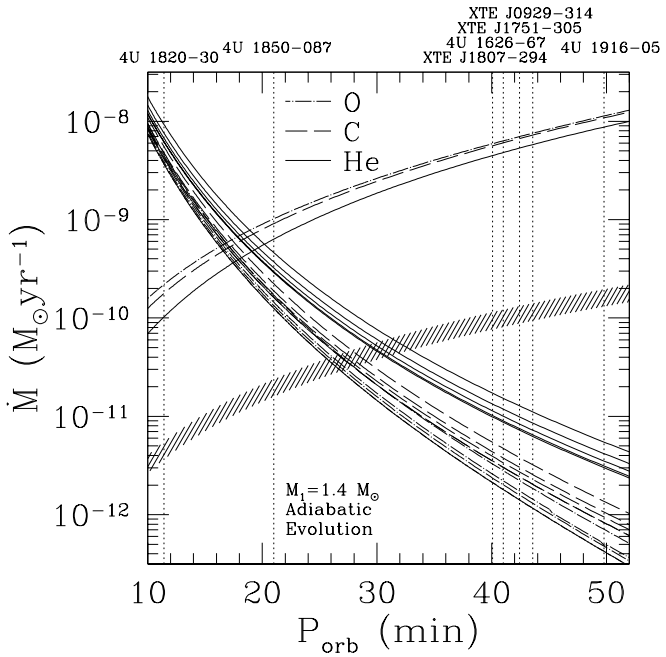

FIG. 11.—$\dot{M}$-$P_{\rm orb}$ relations along adiabatic evolutionary tracks. Each track starts with a donor filling its RL at $P_{\rm orb} = 10$ minutes. For each composition—He (*solid lines*), C (*dashed lines*), and O (*dot-dashed lines*)—tracks for models with initial $T_c = 10^2$, 3×10^5, 2×10^6, 5×10^6, and 10^7 K are shown (*bottom to top*). By the time these systems have evolved to $P_{\rm orb} > 30$ minutes, $\dot{M} \lesssim 10^{-10}\ M_\odot\ {\rm yr}^{-1}$; donors in binaries with $P_{\rm orb} \gtrsim 30$ minutes that have persistent $\dot{M}$-values higher than this cannot have adiabatically evolved from $P_{\rm orb} \leq 10$ minutes. The vertical dotted lines show the orbital periods for ultracompact systems with an NS primary. For each composition, the upward-sloping lines show the critical $\dot{M}$ below which the accretion disk is thermally unstable ignoring irradiation (Menou et al. 2002). The shaded horizontal band gives the critical $\dot{M}$ for an irradiated disk (Dubus et al. 1999) for a range of irradiation efficiencies. The band corresponds to the range of values for the Dubus et al. (1999) C parameter of ±50% the fiducial value.

$\dot{M} > 2 \times 10^{-10}\ M_\odot\ \mathrm{yr}^{-1}$; Chakrabarty et al. 1997) and 4U 1916−05 ($P_{\rm orb} = 49.8$ minutes, $\dot{M} \approx 5 \times 10^{-10}\ M_\odot\ \mathrm{yr}^{-1}$; Swank, Taam, & White 1984). If these measured $\dot{M}$-values reflect the long-term average $\dot{M}$-value, then the donors must be extremely hot ($>10^7$ K; see Fig. 10). However, the typical $\dot{M}$-values at these orbital periods are below where a He or C/O disk is thermally stable (see Fig. 11; Menou et al. 2002; Dubus et al. 1999). In that case, we would explain the present $\dot{M}$-value as a higher rate indicative of a system in outburst. Indeed, the luminosity from 4U 1626−67 is observed to be in a steady slow decline (Mavromatakis 1994; Chakrabarty et al. 1997).

If the ultracompact binaries evolve adiabatically, we can determine their relative numbers as a function of $P_{\rm orb}$. Defining $N(P_{\rm orb})$ such that $N\,dP_{\rm orb}$ is the number of systems with orbital period between $P_{\rm orb}$ and $P_{\rm orb} + dP_{\rm orb}$ and demanding continuity gives

$$\frac{d(N\dot{P}_{\rm orb})}{dP_{\rm orb}} = 0\ , \tag{20}$$

leading to the expected relation between $\dot{P}_{\rm orb}$ and N:

$$\frac{N}{N_0} = \frac{\dot{P}_{\rm orb,0}}{\dot{P}_{\rm orb}}\ , \tag{21}$$

where N_0 and $\dot{P}_{\rm orb,0}$ are the respective quantities at some reference orbital period, $P_{\rm orb,0}$. For $n_{\rm ad}$ fixed, $R \propto M^{n_{\rm ad}}$, and with $M_2 \ll M_1$, equations (15), (16), and (21) lead to the simple relation

$$\frac{d\ln N}{d\ln P_{\rm orb}} = \frac{d\ln \dot{P}_{\rm orb}}{d\ln P_{\rm orb}} = \alpha \equiv \frac{11/3 - 5n_{\rm ad}}{1 - 3n_{\rm ad}}\ . \tag{22}$$

In this case

$$\frac{N}{N_0} = \left(\frac{P_{\rm orb}}{P_{\rm orb,0}}\right)^{\alpha}\ , \tag{23}$$

and from this it is clear that $n_{\rm ad}$ *alone* determines the number distribution. As α increases with $n_{\rm ad}$, systems with C/O donors will have a stronger increase in N with $P_{\rm orb}$ than those with He donors because of the difference in $n_{\rm ad}$ shown in Figure 8. In the more general case, $n_{\rm ad}$ is variable and equation (22) becomes, up to terms of order M_1/M_2,

$$\frac{d\ln N}{d\ln P_{\rm orb}} = \frac{11/3 - 5n_{\rm ad}}{1 - 3n_{\rm ad}} + \frac{18}{(3n_{\rm ad}+5)(3n_{\rm ad}-1)}\,\frac{dn_{\rm ad}}{d\ln P_{\rm orb}}\ , \tag{24}$$

and in general the distribution is almost solely a function of $n_{\rm ad}$.

While equations (22) and (24) highlight the centrality of $n_{\rm ad}$ in determining N, to calculate N for each of the adiabats in Figure 11 it is more straightforward, and slightly more accurate because of the small dependence of N on M_2/M_1, to calculate $\dot{P}_{\rm orb}$ numerically and evaluate equation (21). We calculate $\dot{P}_{\rm orb}$ from

$$\dot{P}_{\rm orb} = -\frac{dP_{\rm orb}}{dM_2}\,\dot{M}_2 = -\frac{P}{2M_2}\,(3n_{\rm ad} - 1)\dot{M}_2\ , \tag{25}$$

where $\dot{M}_2 = -\dot{M}$. We display the resulting N-distribution for each adiabatic track, normalized to the value of N_0 at $P_{\rm orb,0} = 10$ minutes, in Figure 12. It is clear that the distribution is a strong function of composition, through the differing values of $n_R = n_{\rm ad}$, but only weakly depends on the entropy of the donor. The entropy dependence of N derives from the fact that $\dot{P}_{\rm orb} \propto M_2$ (eqs. [15], [17], and [24]) and donors with a higher entropy at a fixed mean density have larger values of M_2 (see Fig. 5). Figure 12 also shows that depending on donor type and entropy, we expect to see roughly 60–160 (for He and C/O donors, respectively) times as many systems at $P_{\rm orb} \approx 40$ minutes than at 10 minutes. While consideration of nonadiabatic evolution will change the value of this ratio, the fact that it will be larger for C/O donors than for He donors is expected to be a robust result, regardless of the evolutionary scenario considered.

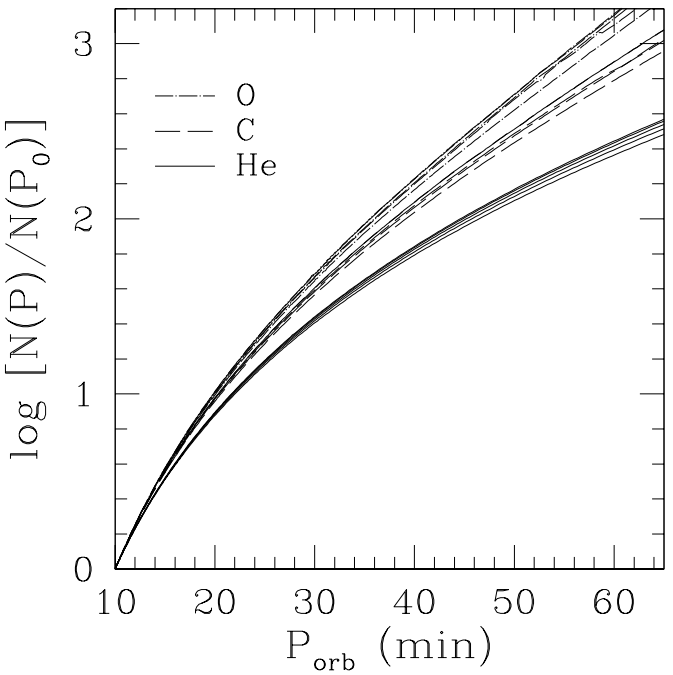

FIG. 12.—Number distribution $N(P_{\rm orb})$ of ultracompact systems along the adiabats shown in Fig. 11. Each distribution is normalized to 1 at $P_{\rm orb} = 10$ minutes. For each composition, from top to bottom, the tracks are for donors with initial $T_c = 10^2,\ 3 \times 10^5,\ 2 \times 10^6,\ 5 \times 10^6$, and 10^7 K. The differences in the distributions between donor types are caused by the differences in their $n_{\rm ad}$ values. The differences in $n_{\rm ad}$ can be seen to play a more significant role in determining $N(P_{\rm orb})$ than those in the initial donor entropy.

5. DISCUSSION AND CONCLUSIONS

We have presented models for arbitrarily degenerate stellar objects including Coulomb physics with masses $M < 0.1\ M_\odot$. At these low masses, the well-known M-R relations for $n = 3/2$ polytropes ($R \propto M$), WDs ($R \propto M^{-1/3}$), and Coulomb-dominated objects ($R \propto M^{1/3}$) merge and transition from one to another. The connection between $T = 0$ degenerate and Coulomb-dominated objects has been found from the Zapolsky & Salpeter (1969) M-R relations. The connection between polytropes and degenerate objects, neglecting Coulomb physics, is seen in the $n = 3/2$ polytropes. Our models make the final connection between the three classes of objects, filling in the gap occupied by $T \neq 0$ objects in which Coulomb physics cannot be neglected.

As discussed in § 2, a ubiquitous feature of stellar M-R relations at sufficiently high values of T_c is the existence of a

minimum mass $M_{\rm min}$ below which equilibrium solutions do not exist. The cause of this is the transition from ideal gas to degenerate electrons providing the pressure support, and we showed in § 2.2 that the well-known maximum T_c in $n = 3/2$ polytropes for a fixed M (Cox & Guili 1968; Rappaport & Joss 1984; Stevenson 1991; Burrows & Liebert 1993; Ushomirsky et al. 1998) is the same physics. The value of $M_{\rm min}$ depends on both T_c (in fact, $M_{\rm min} = 0$ at sufficiently low T_c) and the strength of Coulomb physics. In general, the lower the value of T_c and the stronger the Coulomb interactions, the smaller the value of $M_{\rm min}$. The existence of an $M_{\rm min}$ may have a profound impact on the evolution of a donor undergoing mass loss. For our He WDs, $M_{\rm min} > 0$ for models with $T_c \gtrsim 10^5$ K. As discussed in Bildsten (2002), the existence of an $M_{\rm min} > 0$ leads to the possibility of disrupting the donor through mass loss. This could be accomplished through stable mass loss down to $M_2 = M_{\rm min}$ or via a mass transfer instability. The latter will occur if the expansion of the donor under mass loss exceeds that of the RL. The entropy input needed to cause this instability and the fate of the donor are the subject of future work.

We have applied our model to the accreting ultracompact MSPs. In XTE J1751−305, the donor must be hot regardless of its composition; in XTE J0929−314 and XTE J1807−294, fully degenerate donors are possible, depending on the composition. From orbital inclination constraints, the probability that XTE J1807−294 can accommodate a He donor is 15%, while for XTE J0929−304 this probability is ≈35%, providing support to the notion that some of these donors are likely C/O WDs (Schulz et al. 2001; Juett et al. 2001; Homer et al. 2002). The evolution of each system will differ depending on the orbital inclination. In particular, how far the system can evolve in $P_{\rm orb}$ in a specified time and the expected $\dot{M}$-$P_{\rm orb}$ relation depends on $\sin i$ through the mass, core temperature, and composition of the donor. In general, the $\dot{M}$-$P_{\rm orb}$ relation is additionally parameterized by the donor T_c and composition. We find that the number distribution of systems as a function of $P_{\rm orb}$, $N(P_{\rm orb})$, is determined by the donor's n_R. The distribution for systems with C/O donors thus varies significantly from those with He donors. In the case of adiabatic evolution, the relative number of systems at 40 minutes to that at 10 minutes is ≈160 for C/O donors and ≈60 for He donors. In addition to the accreting MSP systems, our models are applicable to the AM CVn binary systems, which are believed to be double-WD binaries with a He donor (Warner 1995). The application of our models to these systems is the subject of current work.

The constant-entropy models we have calculated give a lower limit on R for a given M, T_c, and composition. The actual thermal profile of a donor will depend on its prior evolution: how entropy is deposited into the star, entropy losses, and how quickly heat transport occurs as compared with mass loss. To determine the entropy profile of a donor in a specific system requires consideration of the coupled evolution of the binary and the donor. While our models do not address this uncertainty, they do provide limiting M-R relations based on the *total* entropy content of the model in a consistent and systematic treatment without consideration of past evolution. As such they will be useful in consideration of binary systems with low-mass WD companions where time evolution of the donor's structure coupled to that of the binary itself is not computationally feasible or necessary. Tracks of our M-R relations and $n_{\rm ad}$ as a function of ρ_c and T_c for He, C, and O donors are available in the electronic edition of the *Journal* as a UNIX tar file.

We thank Deepto Chakrabarty, Craig Markwardt, Gijs Nelemans, and Ira Wasserman for insightful and productive comments and discussions over the course of this work. This work was supported by the National Science Foundation through grants PHY 99-07949 and AST 02-05956 and by NASA through grant NAG5-8658. L. B. is a Cottrell Scholar of the Research Corporation.

REFERENCES

Althaus, L. G., & Benvenuto, O. G. 1997, ApJ, 477, 313
Angelini, L., White, N. E., Nagase, F., Kallman, T. R., Yoshida, A., Takeshima, T., Becker, C., & Paerels, F. 1995, ApJ, 449, L41
Bildsten, L. 2002, ApJ, 577, L27
Burrows, A., Hubbard, W. B., Lunine, J. I., & Liebert, J. 2001, Rev. Mod. Phys., 73, 719
Burrows, A., & Liebert, J. 1993, Rev. Mod. Phys., 65, 301
Chabrier, G., & Potekhin, A. Y. 1998, Phys. Rev. E, 58, 4941
Chakrabarty, D. 1998, ApJ, 492, 342
Chakrabarty, D., et al. 1997, ApJ, 474, 414
Cox, J. P., & Guili, R. T. 1968, Principles of Stellar Structure (New York: Gordon & Breach)
Cox, J. P., & Salpeter, E. E. 1964, ApJ, 140, 485
Dewi, J. D. M., Pols, O. R., Savonije, G. J., & van den Heuvel, E. P. J. 2002, MNRAS, 331, 1027
Driebe, T., Blöcker, T., Schönberner, D., & Herwig, F. 1999, A&A, 350, 89
Dubus, G., Lasota, J., Hameury, J., & Charles, P. 1999, MNRAS, 303, 139
Farouki, R. T., & Hamaguchi, S. 1993, Phys. Rev. E, 47, 4330
Fedorova, A. V., & Ergma, E. V. 1989, Ap&SS, 151, 125
Fontaine, G., Brassard, P., & Bergeron, P. 2001, PASP, 113, 409
Galloway, D. K., Chakrabarty, D., Morgan, E. H., & Remillard, R. A. 2002, ApJ, 576, L137
Hansen, C. J., & Sprangenberg, W. H. 1971, ApJ, 168, 71
Hayashi, C., & Nakano, T. 1963, Prog. Theor. Phys., 30, 460
Homer, L., Anderson, S. F., Wachter, S., & Margon, B. 2002, AJ, 124, 3348
Iben, I., Jr., & Tutukov, A. V. 1985, ApJS, 58, 661
Juett, A. M., Psaltis, D., & Chakrabarty, D. 2001, ApJ, 560, L59
Lai, D., Abrahams, A. M., & Shapiro, S. L. 1991, ApJ, 377, 612
Landau, L. D., & Lifshitz, E. M. 1962, The Classical Theory of Fields (2d ed.; Oxford: Pergamon)
Levine, A., Ma, C. P., McClintock, J., Rappaport, S., van der Klis, M., & Verbunt, F. 1988, ApJ, 327, 732
Markwardt, C. B., Juda, M., & Swank, J. H. 2003a, IAU Circ. 8095
Markwardt, C. B., Smith, E., & Swank, J. H. 2003b, IAU Circ. 8080
Markwardt, C. B., Swank, J. H., Strohmayer, T. E., in 't Zand, J. J. M., & Marshall, F. E. 2002, ApJ, 575, L21
Mavromatakis, F. 1994, A&A, 285, 503
Menou, K., Perna, R., & Hernquist, L. 2002, ApJ, 564, L81
Middleditch, J., Mason, K. O., Nelson, J. E., & White, N. E. 1981, ApJ, 244, 1001
Nelemans, G., Portegies Zwart, S. F., Verbunt, F., & Yungelson, L. R. 2001, A&A, 368, 939
Nelson, L. A., & Rappaport, S. A. 2003, ApJ, 598, 431
Nelson, L. A., Rappaport, S. A., & Joss, P. C. 1986, ApJ, 304, 231
Paczyński, B. 1967, Acta Astron., 17, 287
———. 1976, in IAU Symp. 73, The Structure and Evolution of Close Binary Systems, ed. P. Eggleton, S. Mitton, & J. Whelan (Dordrecht: Reidel), 75
Panei, J. A., Althaus, L. G., & Benvenuto, O. G. 2000, A&A, 353, 970
Podsiadlowski, Ph., Rappaport, S., & Pfahl, E. D. 2002, ApJ, 565, 1107
Potekhin, A. Y., Baiko, D. A., Haensel, P., & Yakovlev, D. G. 1999, A&A, 346, 345
Potekhin, A. Y., & Chabrier, G. 2000, Phys. Rev. E, 62, 8554
Rappaport, S., & Joss, P. C. 1984, ApJ, 283, 232
Rappaport, S., Joss, P. C., & Webbink, R. F. 1982, ApJ, 254, 616
Rasio, F. A., Pfahl, E. D., & Rappaport, S. 2000, ApJ, 532, L47
Salaris, M., García-Berro, E., Hernanz, M., Isern, J., & Saumon, D. 2000, ApJ, 544, 1036
Salpeter, E. E., & Zapolsky, H. S. 1967, Phys. Rev., 158, 876
Savonije, G. J., de Kool, M., & van den Heuvel, E. P. J. 1986, A&A, 155, 51
Schulz, N. S., Chakrabarty, D., Marshall, H. L., Canizares, C. R., Lee, J. C., & Houck, J. 2001, ApJ, 563, 941
Serenelli, A. M., Althaus, L. G., Rohrmann, R. D., & Benvenuto, O. G. 2001, MNRAS, 325, 607
Stevenson, D. 1991, ARA&A, 29, 163
Swank, J. H., Taam, R. E., & White, N. E. 1984, ApJ, 277, 274

Tauris, T. M. 1996, A&A, 315, 453
Ushomirsky, G., Matzner, C. D., Brown, E. F., Bildsten, L., Hilliard, V. G., & Schroeder, P. C. 1998, ApJ, 497, 253
Verbunt, F. 1993, ARA&A, 31, 93
Warner, B. 1995, Ap&SS, 225, 249
Yungelson, L. R., Nelemans, G., & van den Heuvel, E. P. 2002, A&A, 388, 546
Zapolsky, H. S., & Salpeter, E. E. 1969, ApJ, 158, 809